Microchemical and surface evaluation of canine tibial plateau leveling osteotomy plates

William M. Lackowski, PhD; Yulia B. Vasilyeva, MS; Richard M. Crooks, PhD; Sharon C. Kerwin, DVM, MS; Donald A. Hulse, DVM

Objective—To determine the microchemical and surface composition of tibial plateau leveling osteotomy (TPLO) plates before and after explantation.

Sample Population—7 TPLO plates surgically removed from host dogs 6 to 54 months after implantation; 2 raw unpolished-and-unpassivated 316L TPLO plates; and 2 heat-treated, polished-and-passivated, and cleaned 316L TPLO plates.

Procedures—Samples were removed by use of standard techniques to ensure the plate surface was not damaged. Sample pieces were dissolved and analyzed by inductively coupled plasma–mass spectrometry (ICP-MS) to determine bulk elemental composition. Other sample pieces were investigated by use of scanning electron microscopy (SEM), energy dispersive spectroscopy (EDS), and x-ray photoelectron spectroscopy (XPS) for determination of sample morphology, near-surface elemental composition, and surface elemental composition, respectively. To investigate the possibility of corrosion in situ, some samples were chemically corroded and analyzed.

Results—ICP-MS confirmed that elemental composition of samples was consistent with 316L stainless steel. The SEM and EDS analyses revealed trace amounts of polishing materials and a nonuniform carbonaceous biofilm on < 1% of the surface area of samples removed from the host dogs. The XPS analysis indicated an increase in the chromium-to-iron ratio on passivated surfaces, with no difference between passivated samples before implantation and after explantation.

Conclusions and Clinical Relevance—Composition of the TPLO plates was consistent with 316L stainless steel. No chemical or topographic changes were detected in TPLO plates that had been implanted in dogs for up to 54 months. A small amount of biofilm was evident on the surface of 2 plates. (*Am J Vet Res* 2007;68:908–916)

Injury of the cranial cruciate ligament remains the most common cause of hind limb lameness in adult large-breed dogs.[1] Popular breeds such as Labrador Retrievers and Rottweilers are commonly afflicted with gradual tearing of the cranial cruciate ligament. Return to function is best accomplished through surgical intervention.[2–7] Numerous techniques have been described to repair stifle joints that have deficiencies of the cranial cruciate ligament.[1,3,5,8] A procedure favored by many small animal surgeons is the TPLO.[7,8] This procedure changes the mechanics of the joint whereby cranial translation is converted to caudal translation, the latter of which is then neutralized by the caudal cruciate ligament. To accomplish the procedure, an osteotomy of the proximal tibial metaphysis is performed, and the tibial plateau is then rotated to a new position and stabilized with a bone plate and screws. A commercially manufactured plate[a] has commonly been used for the TPLO stabilization. In the past few years, a possible increase in osteosarcoma in dogs that had undergone a TPLO procedure was suggested in a report.[9,11]

Furthermore, issues have been raised regarding the quality of that commercially available TPLO plate (ie, it may not meet established specifications, especially standards for surgical implants). For example, investigators in 1 study[10] reported that intra- and extracellular particulate debris were detected in tissues samples obtained adjacent to the site of TPLO plates and concluded that this debris and mononuclear cell infiltrates observed were probably the result of corrosion. The same group of investigators also implicated the commercially available TPLO plate as a cause of neoplasia in a dog.[11]

Abbreviations

TPLO	Tibial plateau leveling osteotomy
ICP-MS	Inductively coupled plasma–mass spectrometry
SEM	Scanning electron microscopy
EDS	Energy dispersive spectroscopy
XPS	X-ray photoelectron spectroscopy

Received June 2, 2006.
Accepted February 16, 2007.
From the Department of Chemistry, College of Science, Texas A&M University, College Station, TX 77842 (Lackowski, Vasilyeva, Crooks); and the Department of Veterinary Small Animal Clinical Sciences, College of Veterinary Medicine and Biomedical Sciences, Texas A&M University, College Station TX 77843 (Kerwin, Hulse). Dr. Lackowski's present address is Center for Nano and Molecular Science and Technology, University of Texas, Austin, TX 78712. Ms. Vasilyeva's present address is USIO Science Services, Texas A&M University, College Station, TX 77845. Dr. Crooks' present address is Department of Chemistry, University of Texas, Austin, TX 78712.
Supported in part by the National Science Foundation (grant No. 0531030).
The authors thank Dr. Michael Pendleton for assistance with analysis of scanning electron microscopy and energy dispersive spectroscopy data and Dr. Robert Taylor for assistance with the inductively coupled plasma-mass spectrometry analysis.
Address correspondence to Dr. Kerwin.

An additional report[12] also revealed an osteosarcoma in the proximal portion of the tibia at the site of a TPLO performed by use of the commercially available TPLO plate. Crevice corrosion has also been reported[13] in 7 explanted TPLO plates, and the investigators in that study concluded that the cast implants were inferior to wrought implants because it appeared that surface irregularities and porosity served as initiation sites for observed corrosion defects.

Osteosarcomas related to implants have been associated with chronic low-grade inflammation, most commonly secondary to loosening of the implant, galvanic corrosion, and low-grade infection.[14–19] Osteosarcoma in a dog associated with a wrought stainless-steel plate has also been reported[20]; in that dog, there was no histologic evidence of implant loosening or infection.

In vivo, 316L stainless steel is capable of a small amount of corrosion, but this corrosion can be limited by proper passivation, implant fixation (to minimize fretting corrosion), and use of materials composed of similar metals (to avoid galvanic corrosion).[21–24] If long-term implantation of the commercially available TPLO plate results in substantial corrosion, chronic inflammation could result in the development of bone tumors at or near the TPLO site. Therefore, the goal of the study reported here was to determine the microchemical and surface composition of commercially available TPLO plates, particularly as they relate to corrosion, before implantation and after explantation from host dogs.

Materials and Methods

Sample population—Three types of commercially available TPLO plates[a] were used in the study reported here. Plates included 2 unpolished, unpassivated 316L stainless-steel blanks, 2 polished-and-passivated plates that were suitable for implantation, and 7 explanted specimens that were removed from host dogs between 6 and 54 months after implantation. Plates were removed from the host dogs during an exploratory arthroscopy performed because the dogs developed a new lameness on the previously operated limb with signs of pain isolated to the stifle joint, and it was suspected that they had late meniscal tears or that the plate may have been the cause of the new pain or lameness.

Explantation of TPLO plates—Removal of in situ TPLO plates was accomplished through a medial incision. Sharp dissection was used to expose the surface of each plate. A combination of sharp and blunt dissection was used to free each plate from soft tissues that encased it. Care was taken to ensure the surface of each plate was not damaged during removal. Screws were removed, and plates were lifted from the surface of the bone. Gross inspection of the soft tissues adjacent to the plate surfaces was completed, and the soft tissues were sutured by use of standard methods. After removal, each plate and the corresponding screws were gently washed with distilled water, dried with a towel, and placed into clean dry plastic containers until analyzed.

Preparation of explanted samples—Explanted samples were prepared for analysis. Prior to analysis, all samples were rinsed with deionized water for 30 seconds, rinsed in isopropyl alcohol for 30 seconds, and then dried under a stream of nitrogen gas until the surface appeared dry. To accommodate the various mounting geometries of the analysis instruments, TPLO plates were mechanically sectioned into pieces (approx 10 × 10 × 5 mm) by use of a rotary diamond saw.

Optical microscopy—Digital micrographs were obtained by use of a digital optical microscope equipped with a variable magnification objective (20× to 600× magnification), integral fiber-optic light source, and charge-coupled device camera. Digital images were saved as 640 × 480 JPG files.

ICP-MS—Analysis by use of ICP-MS provides information about the elemental composition of the bulk metal from which plates are constructed. Samples were weighed and then digested in aqua regia (HNO_3:HCl [1:4]).[b,c] After digestion for 24 hours, samples were diluted with a weak nitric acid[b] solution (HNO_3:H_2O[d][1:1,000]). Samples were then analyzed with a mass spectrometer[e] fitted with a quadrupole mass filter. Each analysis represented the mean of 10 averaged measurements. To eliminate potential effects of interference from the sample matrix, 5 calibration standards were prepared from separate elemental standards to approximate the concentrations in 316L stainless steel; specifications for the calibration standards were as indicated in a guidance document.[25] Aluminum was added to these calibration standards to ensure that, when necessary, it would be detected and quantified. These 5 standards were then used to construct the calibration curve used to determine concentrations of the samples. The 5 standards were analyzed immediately before and after the samples to ensure consistency in measurements.

SEM and EDS—Scanning electron micrographs were obtained on a scanning electron microscope[f] fitted with a liquid nitrogen–cooled Princeton gamma tech EDS system and on a scanning electron microscope[g] fitted with an in-lens annular detector and a thermal field-emitter source. All images were acquired by use of an accelerating voltage of 15 kV and a working distance of 10 mm. The EDS spectra were integrated for 60 or 100 seconds (scanning electron microscope[f] fitted with the EDS system or the scanning electron microscope[g] fitted with the in-lens annular detector and thermal field-emitter source, respectively) to achieve a high signal-to-noise ratio. Identification of the EDS peaks was determined by use of commercially available software.[h] Use of EDS provided data on elemental analysis of stainless steel (density of 8 g/cm^3) to a depth of approximately 3 μm by use of an accelerating voltage of 15 kV.

XPS—Data for XPS provided elemental analysis of only the top few nanometers of a plate surface. The XPS data were obtained with a commercially available system[i] by use of an Al kα anode source operating at 200 W. Detector pass energy was set at 80 eV, and datum points were collected at 0.5-eV intervals. Each spectrum represented the mean of three 180-second acquisitions. Base pressure in the analysis chamber was $< 5 \times 10^{-9}$ torr for all analyses. Calibration of the energy scale was accomplished for each sample by setting the carbon 1s

electron orbital peak to 284.8 eV; the letter s (and also p, d, and f) refers to the spectroscopist designation for atomic subshells.

Intentional corrosion—To ensure that any corrosion on the explanted plates would be detected, 2 polished-and-passivated TPLO plates were intentionally corroded (oxidized) by exposure to hydrochloric acid for 30 minutes. These plates were prepared by immersion in a polytetrafluoroethylene-coated beaker[j] that contained concentrated hydrochloric acid heated to 65°C. After exposure to the acid, the plates were thoroughly rinsed in deionized water and placed under a stream of nitrogen gas until dry. These plates were then

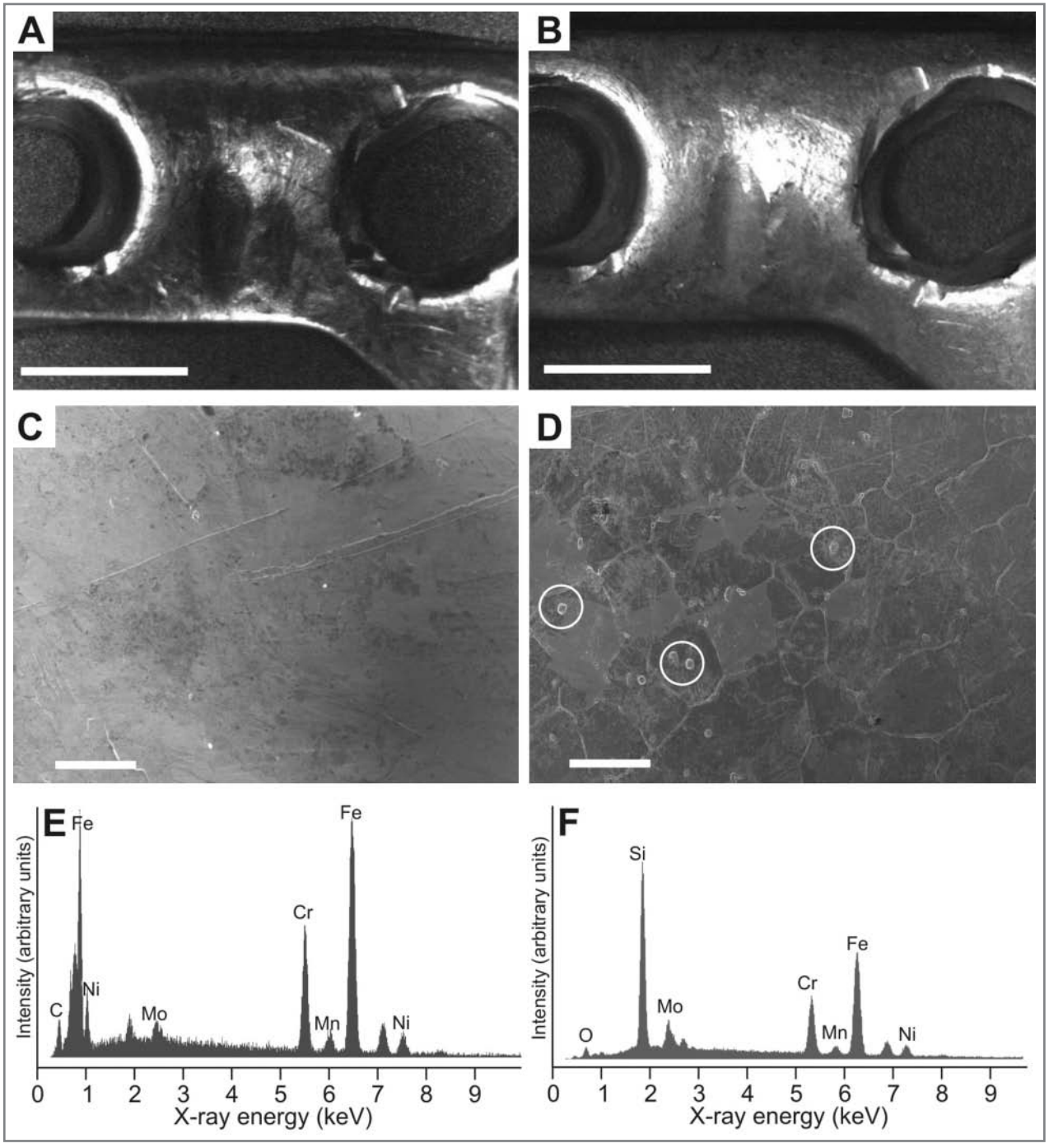

Figure 1—Photomicrographic views (A and B), SEM images (C and D), and EDS spectra (E and F) of a commercially available TPLO plate removed 12 months after implantation (A, C, and E) and following acid-induced corrosion after explantation (B, D, and F). Panels A, C, and E were obtained from the same locations as for panels B, D, and F, respectively. In panels A and B, the depression between the compression holes resulted from manipulation by the surgeon to contour the plate to the bone surface. Panels C and D are SEM images obtained from the depression between the compression holes. In panel D, notice the small corrosion-induced pits (circles). Panels E and F represent an EDS trace obtained at the center of the depression between the compression holes to reveal the content of carbon (C), Fe, Ni, Mo, Cr, Mn, and oxygen (O). Bars in panels A and B = 5 mm; bars in panels C and D = 20 μm.

analyzed by use of the same SEM and EDS procedures as described previously.

Results

The surface of the unpolished plates had a dull metallic matte appearance, which is in contrast to the mirror-like finish after polishing and passivation. An optical micrograph was obtained of a polished-and-passivated plate explanted after 12 months in situ (**Figure 1**). This plate, as well as all the other explanted plates, was quite similar in appearance to polished-and-passivated plates before implantation. At this qualitative level, the only substantial difference between explanted and unused plates was the change in plate morphology that resulted from manipulations performed by the implanting surgeon to conform the plate to the surface of the tibial metaphysis. These manipulations changed the overall shape of the TPLO plate to differing degrees and also introduced small concave indentations as a result of local compression caused by the metal used to bend the plate. Additionally, the surface of 2 of the 7 explanted plates used in the study had small (< 1 mm^2) spots of a reddish-brown film. These spots were only apparent near the compression holes on the convex surface of the plates. Use of SEM and elemental analysis by use of EDS confirmed that these films were composed primarily of carbon (**Figure 2**).

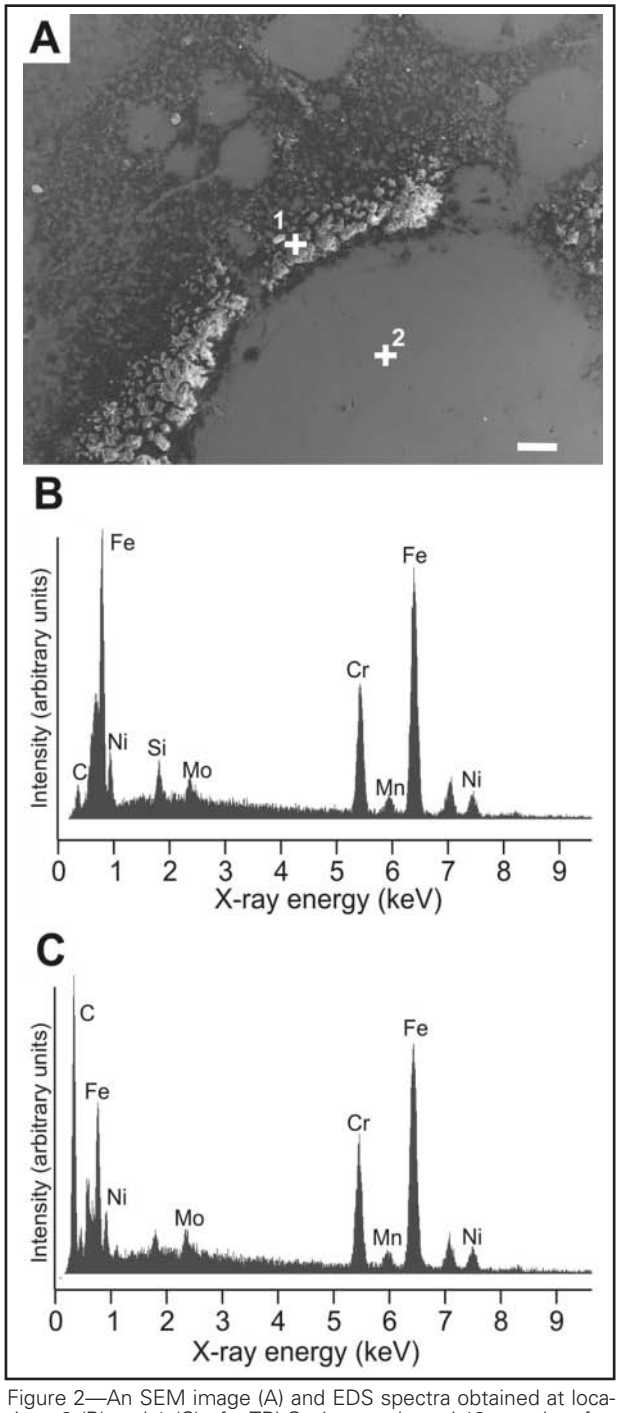

Figure 2—An SEM image (A) and EDS spectra obtained at locations 2 (B) and 1 (C) of a TPLO plate explanted 12 months after implantation. In panel B, the EDS spectrum revealed an expected composition of 316L stainless steel. In panel C, the EDS spectrum revealed a carbon biofilm on the surface of the plate; a biofilm such as this represented an extremely (< 1%) small percentage of the total surface area of the explanted plate. Bar = 40 µm. *See* Figure 1 for remainder of key.

The ICP-MS was used to determine the elemental composition of the TPLO plates. To achieve representative quantitative results, we chose to completely dissolve 1-cm sections of the plates, dilute the resulting solution, and then perform ICP—MS analysis on aliquots of the diluted solution. Complete dissolution of the plate samples required 2 acid-digestion steps. Specifically, a small amount of undissolved gelatinous material remained after the initial 24-hour digestion in aqua regia. It was not possible to isolate the gelatinous material by filtration for direct analysis. Accordingly, 0.1 mL of 49% hydrofluoric acid was added to the original solution, and this treatment completely dissolved the remaining gelatinous material within 30 seconds and yielded a precipitate-free, homogeneous solution. Because this material was insoluble in aqua regia but dissolved readily in hydrofluoric acid, it was considered likely to have been a silica gel arising from the small amount of silicon contained in 316L stainless steel.

Elemental percentages of Fe, Cr, Ni, Mo, Mn, and Al obtained by ICP-MS analysis were summarized (**Table 1**). Although Al is not a component of 316L stainless steel, we conducted an analysis to measure the Al content because it has been reported[10] that Al can be a potentially problematic impurity in implant materials. We did not attempt to quantify the amount of carbon, silicon, phosphorus, and sulfur because they are trace elements in 316L stainless steel. All of the major elements comprising 316L stainless steel were found within the range specified in the guidance document, except for Ni.[25] Nickel content was below the specified range by 3.0% and 3.6% in the polished and unpolished plates, respectively, and by a mean of 6.1% in the 7 explanted TPLO plates.

Although SEM provides high-resolution images of the microstructure of the surface of TPLO plates, it provides a limited field of view; thus, it was not possible to obtain an SEM image of the entire surface of the plates. Therefore, to obtain a characteristic representation of the surface morphology, a minimum of 10 images were obtained for each plate from a number of locations widely distributed over the surface of each plate. Even

Table 1—Elemental composition of commercially available TPLO plates[a] and standards[23] for cast 18 Cr–12.5 Ni–2.5 Mo stainless steel for surgical implants.

Sample	Fe (%)	Cr (%)	Ni (%)	Mo (%)	Mn (%)	Al (%)
Standard	61.65–72.00	17.00–19.00 (0.20)	11.00–14.00 (0.15)	2.00–3.00 (0.10)	0.00–2.00 (0.04)	0*
Unpolished-and-unpassivated (n = 2)	68.30	18.66	10.62	2.39	0.55	0*
Polished-and-passivated (n = 2)	68.27	18.58	10.68	2.38	0.58	0*
Explanted (n = 7)						
1	67.19	18.15	11.91	2.60	0.83	0*
2	68.13	18.87	10.05	2.52	0.97	0*
3	67.70	18.93	10.33	2.62	1.01	0*
4	67.61	19.07	10.23	2.62	1.02	0*
5	68.59	18.56	9.68	2.67	1.09	0*
6	67.45	19.03	10.34	3.13	1.09	0*
7	68.30	18.77	10.03	2.05	0.95	0*

Values reported represent the mean of 10 separate ICP-MS measurements, except for explanted plates 6 and 7, which represent the mean of 5 ICP-MS measurements. All variations were $< \pm 0.1\%$. Because the percentage of each element was determined by a calibration curve created by use of known standards, the totals for each plate may not sum to exactly 100%. Values in parentheses represent the tolerance. *The amount of Al in the sample was less than the limit of detection for ICP-MS.

at magnifications as high as 2,000X, the surfaces of similar plates were remarkably uniform in appearance.

Unpolished TPLO plates had a rough appearance in SEM micrographs. In contrast, polished-and-passivated plates had much smoother surfaces (**Figure 3**). The surface of polished plates was generally flat, but some irregular features (5 µm in diameter) were also observed. The EDS analysis indicated that flat regions of the surface were characterized by elements associated with 316L stainless steel. However, the small irregular features contained Al and oxygen.

Control experiments were performed to intentionally corrode small sections of the surface of several TPLO plates (unpolished and polished blanks and an explanted TPLO plate) by exposing them to concentrated hydrochloric acid for 30 minutes. A low-resolution optical micrograph was obtained for the explanted TPLO plate after acid-induced corrosion (Figure 1). At that low resolution, the surface appeared slightly more reflective than it did prior to corrosion, but there were no other obvious changes. However, at a higher resolution, substantial differences were apparent. Specifically, after acid-induced corrosion, an interconnected network of channels was apparent on the surface of the explanted plate, which represented selective corrosion at the grain boundaries of the stainless steel. Also, numerous small corrosion-induced pits were evident. The EDS data obtained from the intentionally corroded plate revealed a prominent oxygen peak, which was not detected prior to acid-induced corrosion. This peak resulted from the corrosion reaction, which led to formation of metal oxides on stainless steel.[26]

The XPS analysis of the outer few nanometers of the TPLO plates was consistent with the expectation that 316L stainless steel would have a thin, native oxide surface. Specifically, XPS results obtained from all samples analyzed were dominated by oxygen (from Fe, Cr, Ni, Mo, and Mn oxides) and carbon peaks (from small amounts of adventitious hydrocarbon in the environment). This was evident for unpolished-and-unpassivated, polished-and-passivated (but not implanted), and explanted TPLO plates (**Figure 4**). Although dominated by oxygen and carbon 1s orbital photoelectron peaks, the analysis yielded information about the metals contained in the TPLO plates. For example, there were high-resolution XPS spectra of the energy range for Fe. The spectrum of an unpolished-and-unpassivated plate revealed the 1 characteristic Fe 2p electron orbital peaks (ie, Fe $2p_{1/2}$ and Fe $2p_{3/2}$ [the 1/2 and 3/2 refer to different electron spin states]); the Fe $2p_{3/2}$ peak was detected at 712 eV, which corresponded to oxidized Fe (Fe^{II} or Fe^{III}) and not reduced Fe (Fe^{0}). However, in the polished-and-passivated (but not implanted) and explanted plates, Fe was barely detectable. This result was anticipated because the passivation process intentionally removes Fe until a Cr-rich grain boundary dominates the surface.[27] Passivation stops once there is a Cr surface. This was clearly evident because the Cr 2p orbital electron peaks were evident only in the passivated plates (not implanted and explanted) but not in the unpolished-and-unpassivated plate. Importantly, when the surface oxide is damaged in vivo, the stainless steel is capable of self-repassivation.[21–23] It is this repassivation process that differentiates stainless steel from mild steel and also limits release of metal ions from implants into the host body.

Discussion

It has been speculated in the orthopedic veterinarian community that there are problems associated with materials in the commercially available TPLO plate. These problems[11–13] include Al in or on the surface of the TPLO plates; elemental composition of the stainless steel in the TPLO plate that is inconsistent with that of the standard[25] for stainless steel used in implants; and concerns that as a TPLO plate matures in vivo, it undergoes corrosive processes (pitting, fretting, or galvanic corrosion).[24,28–32] Accordingly, the study reported here was conducted to address these 3 issues by analyzing

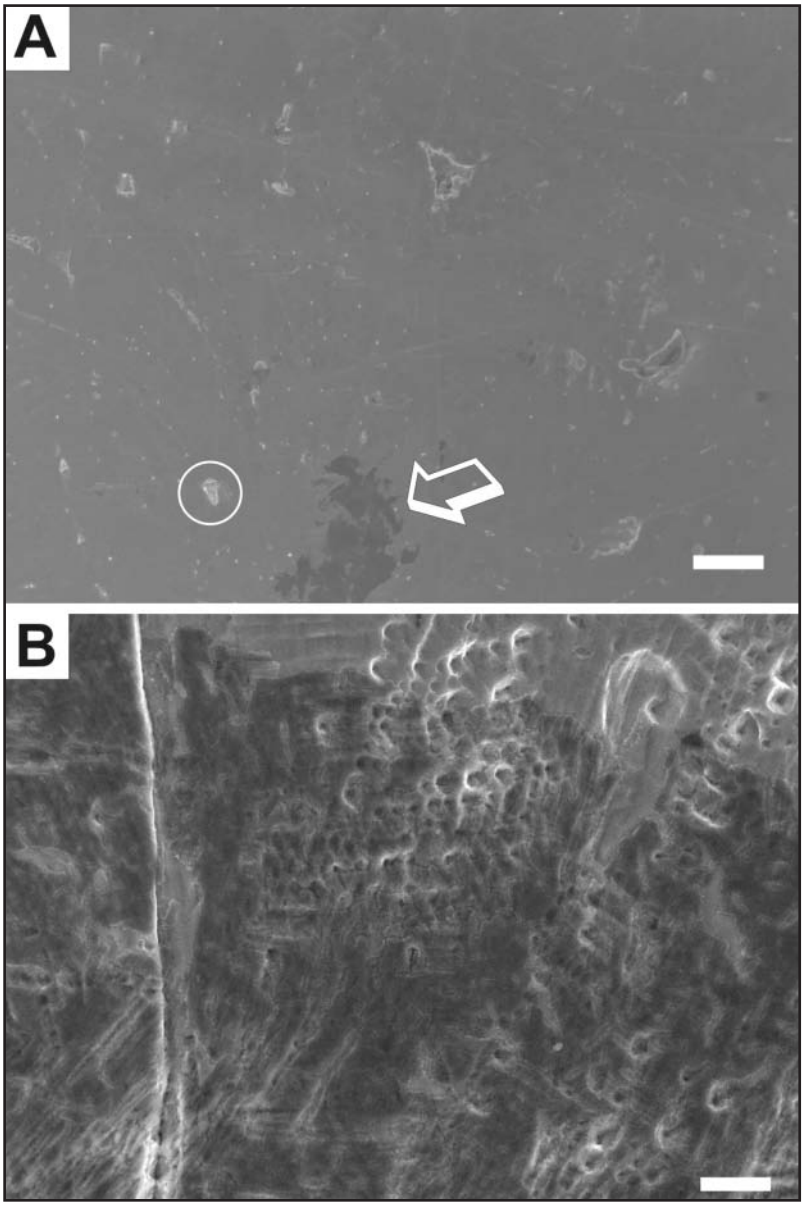

Figure 3—Scanning electron microscopic images of a polished-and-passivated TPLO plate before (A) and after (B) acid-induced corrosion. In panel A, notice the nearly featureless surface of the plate. An EDS analysis confirmed that the near-surface elemental composition was consistent with 316L stainless steel, except for a region composed of Al and oxygen (circle). There is a region of the surface that was slightly darker in appearance (arrow); however, EDS analysis confirmed that this region was elementally similar to the remainder of the TPLO plate. In panel B, the intentionally corroded surface is dominated by pits formed by etching of the individual metal grains. Bars = 25 µm.

the materials and surface properties of TPLO plates. We used 3 types of plates in the study (unpassivated-and-unpolished TPLO 316L stainless-steel plates, passivated-and-polished plates intended for implantation, and passivated-and-polished plates that had been surgically removed from host animals 6 to 54 months after implantation).

Our strategy to determine the compositional structure of the plates involved chemical analysis for 3 depth scales. First, complete acid digestion and analysis by ICP-MS provided elemental analysis of the entire plate. Second, SEM and EDS provided the elemental composition of approximately the outer 3 µm of the plates.[33] Third, XPS provided information about the elemental composition and oxidation state of approximately the outer 3 nm of the plate surface.[34]

In addition to differences in depth resolution, XPS and the combination of SEM and EDS provided 2- and 1-µm spatial resolution in the plane of the plate surface, respectively. Our multiple-scale analysis approach did not reveal Al in the TPLO plates. The ICP-MS analysis indicated that there was no Al contained in the plates. Analysis by use of SEM and EDS indicated that there was some Al on the surface of the plates. This Al signal was accompanied by an oxygen signal. The Al and oxygen most likely were in the form of inert alumina (Al_2O_3) polishing particles that remained on the surface. These remaining polishing particles are much harder than stainless steel (hence, the reason they are used as a polishing medium), and therefore they can become embedded within the surface of a plate. Additional evidence that the particles were residual polishing medium was the fact that their size and shape were consistent with the polishing media used on TPLO plates. Furthermore, these particles were not found on the unpolished plates. It also appears that once these particles become embedded on the metal surface, they are not dislodged while the implant is in the host body (ie, the surface density of these particles was similar regardless of time until explantation).

The perception that the commercially available TPLO plates are constructed from an alloy that does not meet the standard for 316L stainless steel was addressed by the ICP-MS experiments. The ICP-MS analysis revealed that the elemental composition of the plate material conformed to the standard specifications, except for the percentage of Ni. The specification for Ni is between 11.00% and 14.00% with a tolerance of 0.15%. Eight of the 9 polished-and-passivated plates used in the study contained Ni content lower than the specification standard of 11.00% (Table 1). Mean Ni content was 10.43% for all plates tested. However, this slightly lower percentage of Ni should not adversely affect corrosion resistance of the stainless steel. A reduction of 0.5% Ni will lower the pitting potential by only 0.001 V.[35] The small decrease in Ni content should slightly affect the ratio of the ferrite phase to the austenitic phase. By use of a Schaeffler diagram,[35,36] a 0.5% change in the Ni content will change the ferrite content from 4% to 6%.

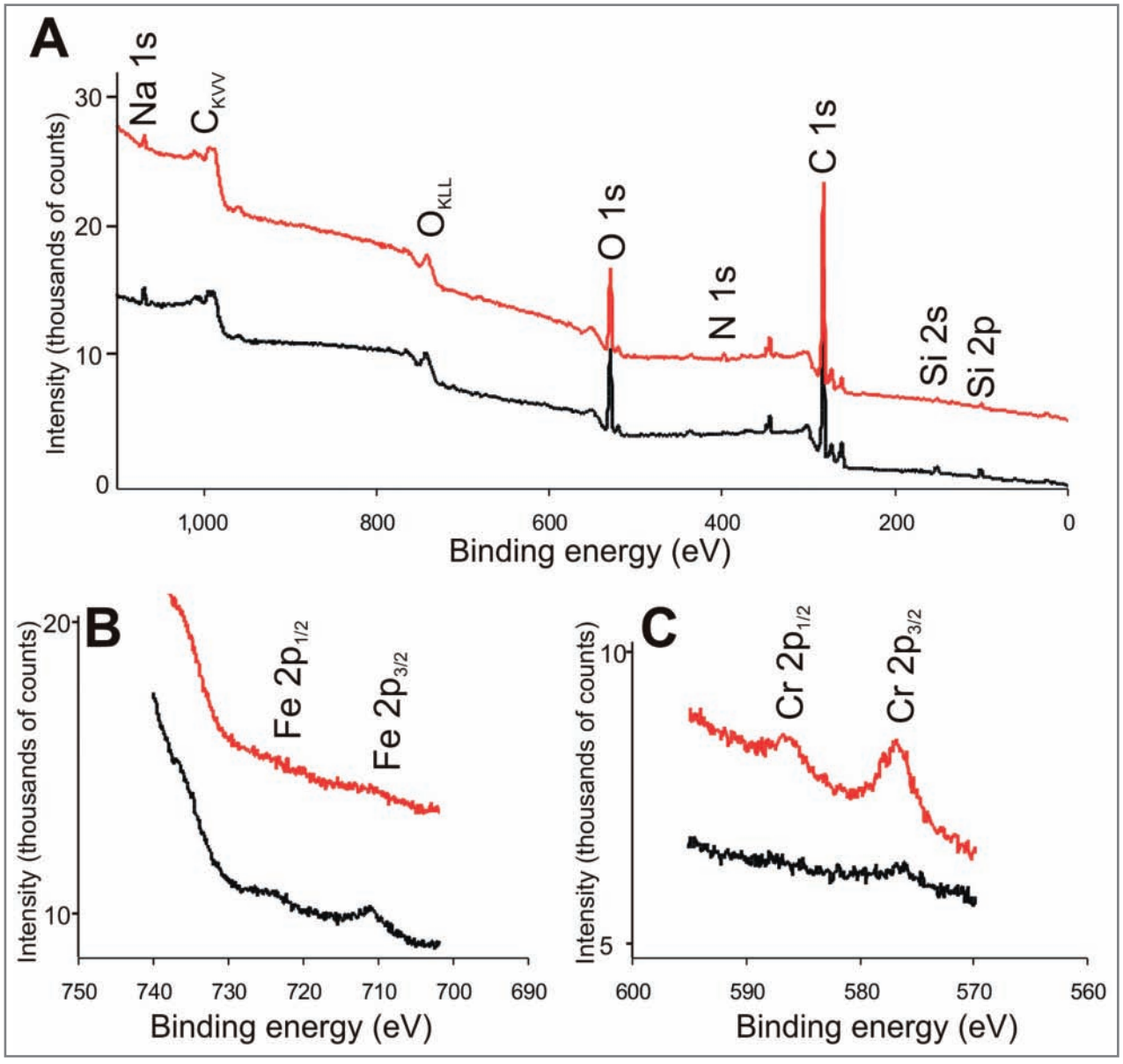

Figure 4—Graphs of XPS analysis of TPLO plates for an unpolished-and-unpassivated plate (black line) and a polished-and-passivated plate (red line; A) and high-resolution XPS scans of the Fe 2p (B) and Cr 2p (C) regions. O = Oxygen. s and p = Spectroscopist designation for atomic subshells. BE = Binding energy. 1/2 and 3/2 = Different electron spin states. KVV and KLL = Designations for the 3 atomic subshells involved in the Auger process.

The change in the amount of δ ferrite was determined by use of the Cr equivalent-to-Ni equivalent ratio calculated by use of the following equation for the Ni and Cr equivalents:

$$\text{Cr equivalent} = \text{Cr} + (1.5 \times \text{silica}) + (1.4 \times \text{Mo}) + \text{Niobium} - [4.99 \times \text{Ni equivalent}]) = \text{Ni} + (30 \times \text{carbon}) + (0.5 \times \text{Mn}) + ([26 \times \{\text{nitrogen} - 0.02\}] + 2.77)$$

The small change in the percentage of possible δ ferrite could slightly alter the mechanical and magnetic properties but not the corrosion resistance.

To address concerns about the possibility that the commercially available TPLO plates corrode in situ, we intentionally corroded TPLO plates so that we could assess the effect of intentional corrosion on each of our analytic techniques. Direct comparison of samples with uncorroded and intentionally corroded surfaces provided an excellent means for assessing evidence of corrosion. Accordingly, small sections of the surface of unpolished-and-unpassivated, polished-and-passivated (but not implanted), and polished-and-passivated explanted plates were intentionally corroded by exposing them to hydrochloric acid. Except for slight differences in reflectivity, the plates did not differ substantially in appearance before or after intentional corrosion. In contrast to these results, it was easy to distinguish differences in the appearance of the surfaces by use of high-resolution SEM. For example, cracks and pits were evident on the intentionally corroded surface but not on the explanted plate that was not intentionally corroded (Figure 1).

Examination of micrographs also revealed obvious differences for the explanted plate. The EDS is particularly useful for distinguishing between corroded and uncorroded plates. Specifically, a high oxygen content, which is characteristic of corrosion products of stainless steel, was found in the EDS spectrum of the intentionally corroded explanted plate but not in the spectrum of the plate that was not exposed to hydrochloric acid (Figure 1).

In 2 explanted plates, a reddish-brown film was detected near the compression holes (Figure 2). Without the benefit of a high-magnification SEM or EDS analysis, these films appeared similar in color and structure to Fe oxide, a corrosion product of stainless steel. However, analysis of the EDS spectra indicated a large amount of carbon in this film but not in the nearby film-free region. Moreover, white areas evident in the regions were believed to arise from electron charging, which is characteristic of an insulating region of the surface, such as a biofilm.[37] Analysis of these results indicated that the structure was a biofilm rather than Fe oxide (detection of Fe oxide would indicate crevice or fretting corrosion). The biofilms were quite similar in appearance to areas interpreted as arising from corrosion in another study[13] of TPLO plates. Similarities in the analysis provided here and in that study[13] include the results of the EDS analysis, including high carbon content, and evidence of electronic charging in the SEM micrographs.

Differences in contrast in SEM images that may have been interpreted as corroded regions of the plate represented topographic features that affected light reflectivity of the microscope (Figure 1). Additionally, there are regions in the SEM images that are indicative of differences in electron scattering, which EDS confirmed to be compositionally identical. One would expect an increase in the amount of oxygen signal in the EDS spectrum of a corroded area.

We have also found that XPS can distinguish differences between raw unpolished plates and those that have been heat treated, polished, passivated, and cleaned. However, its extreme surface sensitivity makes it difficult to analyze the metal underlying the oxide and adventitious hydrocarbons. One conclusion that can be reached from the XPS results is that the passivation procedure used to generate a stable Cr oxide surface was accomplished and this passivation layer did not degrade while the implant was in situ for up to 54 months.

The commercially available TPLO plates analyzed are cast (as opposed to wrought) 316L stainless-steel plates. Although wrought materials are the accepted standard for many bone-stabilization implants, TPLO plates require bending to conform to the bone, and the greater malleability of a cast implant provides a distinct advantage. We were unable to find any evidence of corrosion on the explanted plates by use of a combination of techniques designed to examine the bulk elemental analysis of the plates (ie, ICP-MS) as well as the surface of the plates (ie, XPS and EDS) at 2 depths. Areas of a reddish-brown film observed near the screw holes in 2 plates, which initially appeared to be consistent with Fe oxide, a corrosion product of stainless steel, were found to be a biofilm during subsequent investigation. We were unable to find evidence of corrosion in the 7 explanted TPLO plates investigated in our study.

a. TPLO bone plate, Slocum Enterprises, Eugene, Ore.
b. Omnitrace Ultra high purity HNO_3, EM Science, Gibbstown, NJ.
c. Omnitrace Ultra high purity HCL, EM Science, Gibbstown, NJ.
d. Academic Water Purifier, Millipore Corp, Billerica, Mass.
e. Perkin-Elmer DRCII ICP-MS, Perkin-Elmer, Waltham, Mass.
f. JEOL JSM-6400, JEOL Ltd Tokyo, Japan.
g. LEO 1530, Leica Microsystems, Bensheim, Germany.
h. Genesis microanalysis software, EDAX, Mahwah, NJ.
i. Kratos Axis Ultra XPS, Kratos Ltd, Manchester, UK.
j. Fisherbrand PTFE Beaker, Thermo Fisher Scientific, Waltham, Mass.

References

1. Whitehair JG, Vasseur PB, Willits NH. Epidemiology of cranial cruciate ligament rupture in dogs. *J Am Vet Med Assoc* 1993;203:1016–1019.
2. Aragon CL, Budsberg SC. Applications of evidence-based medicine: cranial cruciate ligament injury repair in the dog. *Vet Surg* 2005;34:93–98.
3. Conzemius MG, Evans RB, Besancon MF, et al. Effect of surgical technique on limb function after surgery for rupture of the cranial cruciate ligament in dogs. *J Am Vet Med Assoc* 2005;226:232–236.
4. Damur DM, Tepic S, Montavon PM. Proximal tibial osteotomy for the repair of cranial cruciate-deficient stifle joints in dogs. *Vet Comp Orthop Traumatol* 2003;16:211–216.
5. Jerram RM, Walker AM. Cranial cruciate ligament injury in the dog: pathophysiology, diagnosis and treatment. *N Z Vet J* 2003;51:149–158.
6. Jerram RM, Walker AM, Warman CGA. Proximal tibial intraarticular ostectomy for treatment of canine cranial cruciate ligament injury. *Vet Surg* 2005;34:196–205.
7. Reif U, Hulse DA, Hauptman JG. Effect of tibial plateau leveling on stability of the canine cranial cruciate-deficient stifle joint: an in vitro study. *Vet Surg* 2002;31:147–154.
8. Shelley BA, Hulse DA, Slater MR, et al. Determination of graft forces for cranial cruciate ligament reconstruction in the dog. *Vet Comp Orthop Traumatol* 1996;9:165–171.
9. Slocum T. Questions accuracy in study of metal plate implants (lett). *J Am Vet Med Assoc* 2006;228:195–196.
10. Boudrieau RJ, McCarthy RJ, Sprecher CM, et al. Material properties of and tissue reaction to the Slocum TPLO plate. *Am J Vet Res* 2006;67:1258–1265.
11. Boudrieau RJ, McCarthy RJ, Sisson RD. Sarcoma of the proximal portion of the tibia in a dog 5.5 years after tibial plateau leveling osteotomy. *J Am Vet Med Assoc* 2005;227:1613–1617.
12. Straw M. What is your diagnosis? Fracture/implant-associated osteosarcoma following TPLO procedures. *J Small Anim Pract* 2005;46:457–459.
13. Charles AE, Ness MG. Crevice corrosion of implants recovered after tibial plateau leveling osteotomy in dogs. *Vet Surg* 2006;35:438–444.
14. Keel SB, Jaffe KA, Nielsen P, et al. Orthopaedic implant-related sarcoma: a study of twelve cases. *Mod Pathol* 2001;14:969–977.
15. Kumar K. Osteosarcoma associated with a metal implant. *Int Orthop* 1996;20:335–336.
16. Roush JK, Kirby BM, Manley PA, et al. Chronic osteomyelitis associated with orthopedic implants and cranial cruciate repair in 3 dogs. *J Am Vet Med Assoc* 1990;196:1123–1126.
17. Li XQ, Hom DL, Black J, et al. Relationship between metallic implants and cancer: a case-control study in a canine population. *Vet Comp Orthop Traumatol* 1993;6:70–74.
18. Murphy ST, Parker RB, Woodard JC. Osteosarcoma following total hip arthroplasty in a dog. *J Small Anim Pract* 1997;38:263–267.
19. Stevenson S. Fracture-associated sarcomas. *Vet Clin North Am Small Anim Pract* 1991;21:859–872.
20. Rose BW, Novo RE, Olson EJ. Osteosarcoma at the site of a triple

pelvic osteotomy in a dog. *J Am Anim Hosp Assoc* 2005;41:327–331.
21. Frangini S, Piconi C. Repassivation rates of surgical implant alloys by rotating-disk scratching measurements. *Werkst Korros* 2001;52:372–380.
22. Weldon LM, McHugh PE, Carroll W, et al. The influence of passivation and electropolishing on the performance of medical grade stainless steels in static and fatigue loading. *J Mater Sci Mater Med* 2005;16:107–117.
23. Gotman I. Characteristics of metals used in implants. *J Endourol* 1997;11:383–389.
24. Okazaki Y, Gotoh E, Manabe T, et al. Comparison of metal concentrations in rat tibia tissues with various metallic implants. *Biomaterials* 2004;25:5913–5920.
25. American Society for Testing and Materials. *ASTM F745–00 standard specification for 18 Cr–12.5 Ni–2.5 Mo stainless steel for cast and solution-annealed surgical implant applications*. Philadelphia: American Society for Testing and Materials, 2000.
26. Salaita G, Tate P. Application of surface and surface imaging techniques in the study of erosion-corrosion in stainless steel. *Corrosion* 1996;52:493–495.
27. American Society for Testing and Materials. *ASTM A380–99 standard practice for cleaning, descaling, and passivation of stainless steel parts, equipment, and systems*. Philadelphia: American Society for Testing and Materials, 1999.
28. Sudhakar KV. Metallurgical investigation of a failure in 316L stainless steel orthopaedic implant. *Eng Failure Anal* 2005;12:249–256.
29. Tutunaru B, Samide A, Preda M. The study of the electrochemical behaviour of 316L stainless steel bioimplants in physiological serum. *Revista Chimie* 2004;55:757–758.
30. Hanawa T. Metal ion release from metal implants. *Mater Sci Eng C* 2004;24:745–752.
31. Duisabeau L, Combrade P, Forest B. Environmental effect on fretting of metallic materials for orthopaedic implants. *Wear* 2004;256:805–816.
32. Sharan D. The problem of corrosion in orthopaedic implant materials. *Orthop Update India* 1999;9:27–31.
33. Ng F. Metallic thin film depth measurements by x-ray microanalysis. *Appl Surf Sci* 2006;252:3972–3976.
34. Briggs D, Seah M. Spectroscopy. In: Briggs D, Seah M, eds. *Practical surface analysis by auger and x-ray photoelectron spectroscopy*. New York: John Wiley & Sons, 1983;120–125.
35. Sedriks AJ. Corrosion of stainless steels. New York: John Wiley & Sons, 1979;71–100.
36. Beddoes J, Parr JG. In: Beddoes J, Parr JG, eds. *Introduction to stainless steels*. 3rd ed. Materials Park, Ohio: ASM International Materials Park, 1999;208.
37. Goldstein J. Electron microscopy. In: Goldstein J, Newbury D, Joy D, et al, eds. *Scanning electron microscopy and x-ray microanalysis*. 3rd ed. New York: Kluwer Academic/Plenum Publishers, 2003;66–72.